R.E.M. (Rekayasa Energi Manufaktur) Jurnal | Vol.8 No.2/2023
ISSN online (2528-3723)
http://doi.org/10.21070/rem.v8i2.1679

Thermodynamic Analysis of Hydrogen Production from Hydrogen Sulfide in Geothermal Power Plant by using Fe-Cl Hybrid Indirect Electrolysis

Putri Nur Fadhilla[1*], Udi Harmoko[2], Marcelinus Christwardana[3]
*Email corresponding author: fadhilla.pu3@gmail.com

[1] Master Program of Energy, School of Postgraduate Studies, Diponegoro University, Indonesia
[2] Department of Physics, Faculty of Science and Mathematics, Diponegoro University, Indonesia
[3] Department of Chemistry, Faculty of Science and Mathematics, Diponegoro University, Indonesia

Article history: Received: 26 June 2023 | Revised: 16 July 2023 | Accepted: 2 August 2023

Abstract. *Clean and sustainable energy sources are needed to meet global energy demand. Geothermal Power Plants (GPPs) may generate power from Earth's heat. However, GPPs release hazardous hydrogen sulfide (H_2S) gas. To overcome this problem and maximize on resource potential, researchers have investigated converting GPP-emitted H_2S into hydrogen (H_2). The Fe-Cl hybrid indirect electrolysis technique is used to analyze the thermodynamics of hydrogen synthesis from H_2S in GPPs. Electrolysis electricity, hydrogen generation rate, and electrolyzer energy and exergy efficiency are examined in the thermodynamic analysis. The foundation parameters show that the electrolysis process uses 20.57 kWh of power every kilogram of H_2 generated. Energy and exergy efficiencies of the electrolyzer are 89.89% and 97.72%, respectively, exhibiting system efficiency. The research also examines how H_2S mass flow rate and electrolysis temperature affect energy efficiency, exergy efficiency, and power consumption. Optimizing hydrogen generation and system performance requires these elements. This study analyzes the thermodynamics of hydrogen synthesis from H_2S in GPPs to create sustainable and ecologically friendly energy options. H_2S emissions from GPPs might be used to efficiently produce hydrogen as a renewable energy source with more research.*

Keywords *- Hydrogen, Hydrogen sulfide, Fe-Cl hybrid, Electrolysis, Geothermal*

INTRODUCTION

Climate change, caused by rising global temperatures, is a global concern. It results in altered rainfall patterns, the loss of habitable coastal land due to rising sea levels, and the thawing of ice sheets and glaciers [1]. In addition, climate change poses health hazards, such as heat-related problems and respiratory illnesses [2]. Consequently, there is an increasing demand for innovative energy transition toward sustainable alternatives, hydrogen (H_2) being one of them.

Hydrogen is considered an environmentally beneficial energy source due to the fact that it emits only water and oxygen [3], [4]. Hydrogen's ability to convert to and from secondary energies such as electricity and heat, its ability to store energy efficiently with a high energy density, and its low flash point, which requires a simple combustion system, are notable advantages [5]. Hydrogen cannot be found naturally because it is extremely reactive and creates covalent bonds with other elements rapidly. Consequently, a production procedure is required.

Hydrogen is utilized in numerous industrial sectors, such as cryogenics, oil and gas, petrochemicals, nuclear power generation, hydrocarbon-based fuel production, aerospace, automotive, and telecommunications [6]. Several methods exist for the production of hydrogen, including natural gas reforming, electrolysis, liquid reforming, nuclear high-temperature electrolysis, high-temperature thermo-chemical water-splitting, photo-biological, and photo-electrochemical processes [7]. Approximately eighty percent of the world's hydrogen production is still dominated by fossil fuels [8]. To remedy this, there is a need for innovation and the production of green hydrogen from renewable energy sources [9]. This strategy not only reduces environmental contamination, but also encompasses the entire production process, storage, distribution, and utilization [10].

In the context of geothermal power plants (GPP), hydrogen can be produced by electrolyzing the GPP's residual water with electricity. Through the liquefaction process, hydrogen can be efficiently stored, facilitating easier distribution and making geothermal energy more economically viable [11]. Extensive research has been conducted on the production of hydrogen from GPP, with an emphasis on the development of technological methods that are efficient and economically viable. Some researchers have also investigated the possibility of producing hydrogen from hydrogen sulfide (H_2S). Approximately 7.72 million tons of H_2S are emitted annually from a variety of sources, including natural processes, biological activities, and industrial processes [12]. Utilizing H_2S in the production of hydrogen and other products with added value can contribute to sustainability and a circular economy. In addition,

Copyright © 2023 Author [s]. This is an open-access article distributed under the terms of the Creative Commons Attribution License (CC BY). The use, distribution or reproduction in other forums is permitted, provided the original author(s) and the copyright owner(s) are credited and that the original publication in this journal is cited, in accordance with accepted academic practice. No use, distribution or reproduction is permitted which does not comply with these terms

the energy cost and voltage requirements for H_2S decomposition and electrolysis are considerably less than those for water decomposition [13]. There have been studies on the potential for hydrogen production from H_2S in integrated gasifier combined cycle (IGCC) power facilities [13], the electrolysis of H_2S in Black Sea water [14], and the exploitation of H_2S from geothermal geothermal areas [15]. These studies demonstrate the economic viability of using H_2S from geothermal sources in the production of hydrogen.

As geothermal fluids contain various non-condensable gases (NCG) in both dissolved and gaseous states, H_2S represents a significant portion of GPP emissions. The NCG is a mixture of carbon dioxide (CO_2), hydrogen sulfide (H_2S), hydrogen (H_2), nitrogen (N_2), methane (CH_4), and argon (Ar) [16]. When turbine steam residue moves towards the condenser, these gases accumulate in the flash and steam systems' condensers, and their presence increases back pressure at the turbine outlet, thereby diminishing turbine performance. Thus, these gases must be released [17]. The NCG and H_2S can be released through the chimney and used for hydrogen production.

Modeling study on the production of hydrogen from H_2S in a GPP equipped with AMIS (abatement for mercury and hydrogen sulfide) technology has been conducted [18]. In the AMIS unit, the captured H_2S is subjected to an electrolysis procedure to break it down into hydrogen and sulfur. This process yielded energy and exergy efficiencies of 27.8% and 57.8%, respectively, under H_2S feed conditions of 150°C. In addition, the required electrical power decreases from 73.7 kW to 58 kW as the H_2S temperature rises from 300 K to 800 K, whereas it rises as H_2S mass flow rates increase. Huang et al., (2019) conducted an additional study on H_2S removal via an indirect electrochemical process employing an acid solution of Fe^{3+}/Fe^{2+} as the electrochemical intermediate. The results indicated an H_2S absorption process efficiency of greater than 99%, with hydrogen production proportional to the amount of H_2S absorbed.

To gain a more thorough understanding of the potential for hydrogen production from H_2S, particularly in GPPs, additional research is required. The purpose of this paper is to examine the effect of H_2S mass flow rate and electrolysis temperature on a variety of factors, including electricity consumption, exergy destruction, entropy generation rate, energy and exergy efficiency, and hydrogen production. We believe that this study will serve as a foundation for future research on hydrogen production from H_2S.

MATERIAL AND METHOD

A. Hydrogen generation from hydrogen sulfide at GPP

Geothermal energy is a renewable and eco-friendly energy source, characterized by its purity [6] and sustainability. This is due to the fact that only a small portion of the available geothermal heat is extracted [20]. However, the use of high enthalpy geothermal systems results in the emission of non-condensable gases (NCG), such as carbon dioxide (CO_2), hydrogen sulfide (H_2S), hydrogen (H_2), nitrogen (N_2), methane (CH_4), and argon (Ar). The amount of non-condensable gases (NCG) in a geothermal system varies based on variables such as the temperature and chemical composition of the soil/rock, fluid circulation rate, and the technology employed [15], [17]. CO_2 remains the predominant gas, followed by H_2S, despite the fact that the proportions of these gases vary among geothermal fields.

In the geothermal power plant (GPP) under study, the NCG content ranged from 0.05% to 0.5% by weight, with a gas composition consisting of 60-70% CO_2, 20-25% H_2S, 0.3-0.7% NH_3, 4-10% N_2, and 0.2-0.5% H_2. H_2S is an odorless gas with a distinct odor resembling rotting eggs. At specific concentrations, H_2S can be hazardous to human health, causing respiratory, nervous, and metabolic disorders. In severe circumstances, it can even be fatal [21], [22]. Nevertheless, by utilizing H_2S, we can mitigate its detrimental effects on the environment and human health. During the GPP process, the H_2S released as part of the NCG can be utilized for hydrogen production.

The GPP analyzed in this study utilizes a combination of flash steam system (steam expander) and binary cycle (brine ORC and steam ORC) technologies. The wet steam ORC is primarily responsible for emissions. Through the NCG vent, the NCG, which includes H_2S, is released into the atmosphere. In order to reduce the negative environmental effects of gas emissions, these gases are captured and converted to hydrogen through an electrolysis process.

There are three methods for electrolyzing H_2S into hydrogen: the direct method, the indirect method, and the high-temperature [23]. In this study, it was determined that the indirect electrolysis technique, specifically the Fe-Cl hybrid method, was the most effective [24]. Since H_2S is one of the gases present in the NCG, it must be isolated from other gases in order to prevent interference with the electrolysis process and maximize hydrogen production. The Fe-Cl hybrid method desulfurizes H_2S-containing gas by absorption in a highly acidic iron solution, followed by electrolysis to regenerate the absorbent and produce hydrogen [25].

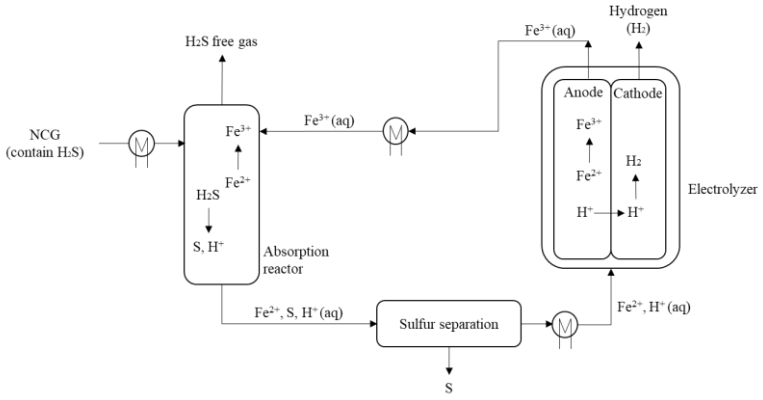

Figure 1. Flowchart for separating H_2S in NCG in an indirect electrolysis process [19]

The following reactions occur throughout the process [19]:

Absorption reaction:
$2Fe^{3+} + H_2S \rightarrow 2Fe^{2+} + 2H^+ + S\downarrow$

Electrolysis reaction:
Anode: $2Fe^{2+} \rightarrow 2Fe^{3+} + 2e^-$
Cathode: $2H^+ + 2e^- \rightarrow H_2\uparrow$
Overall reaction: $H_2S \rightarrow H_2\uparrow + S\downarrow$

The procedure includes three major steps: chemical absorption of H_2S, separation of sulfur precipitates, and electrolysis to regenerate the absorbent and produce hydrogen. Hydrogen sulfide gas from the NCG reacts with Fe^{3+} ions in an acid solution to produce sulfur precipitates and H^+ ions in the absorption reactor. Fe^{3+} ions are simultaneously reduced to Fe^{2+} ions. At the optimal temperature of 70°C, approximately 99% of H_2S can be removed from the material [24], [25]. Due to the 30°C temperature of the NCG emitted from the GPP's NCG exhaust, a heat exchanger unit is required for optimal separation results. Sulfur can be separated using either physical or chemical techniques.

During electrolysis, Fe^{2+} ions are oxidized to Fe^{3+} ions at the anode, while hydrogen protons travel through the proton exchange membrane and are reduced to hydrogen at the cathode. Given the intensely acidic conditions of the reaction, the electrode of the electrolytic cell must be composed of acid-resistant materials such as graphite or carbon fiber [25]. The quantity of hydrogen produced is theoretically equal to the amount of H_2S absorbed [19].

Electrolysis of H_2S was performed with a PEM (Proton Exchange Membrane) electrolyzer. This type of electrolyzer utilizes a dense membrane that separates the anode and cathode chambers and facilitates proton conduction. PEM electrolyzers are renowned for their high productivity and efficiency [18]. Typically, they rely on renewable energy sources to store and provide energy on demand or to transport energy in the form of hydrogen over long distances [26].

B. Thermodynamic Analysis

By calculating energy and exergy, the thermodynamic performance of the electrolyzer is quantitatively analyzed. The analysis is performed on the basis of the following assumptions:

- It is presumed that the ambient temperature (T_0) and pressure (P_0) are 25°C and 101.32 kPa, respectively.
- Throughout the procedure, all fluxes and components maintain constant temperature and pressure.
- It is presumed that the system is in a steady-state and steady-flow condition.
- Potential and kinetic energy fluctuations are considered negligible.
- All gases are presumed to behave as ideal gases.
- There is negligible heat transfer between the system and its environs.
- Additional components are adequately insulated and able to conduct electricity without incurring losses.
- It is assumed that the percentage of H_2S in the NCG is stable, extending from 20% to 25%.

During electrolysis, Fe^{2+} ions are oxidized to Fe^{3+} ions at the anode, while hydrogen protons travel through the proton exchange membrane and are reduced to hydrogen gas at the cathode. The quantity of hydrogen produced is theoretically equal to the amount of H_2S absorbed [19], as described by the previously mentioned chemical reaction.

Analyzing mass, energy, and exergy balances for chemically reacting steady-flow systems constitutes the thermodynamic analysis of the hydrogen production process. The following equations are utilized in these calculations, which are founded on the aforementioned assumptions.
The mass balance of the electrolysis operation for producing hydrogen from H_2S can be expressed as follows:

$$\sum \dot{n}_R = \sum \dot{n}_P \quad (1)$$

$$\dot{n}_{FeCl_2} + \dot{n}_{HCl} = \dot{n}_{FeCl_3} + \dot{n}_{H_2} \quad (2)$$

Before writing the energy balance equation, the enthalpies of the components involved in a system's reaction must be stated. The enthalpy of a component is expressed in mole basis units as follows [27]:

$$Enthalpy = \bar{h}^{\circ}f + (\bar{h} - \bar{h}^{\circ}) \qquad (kJ/mol) \quad (3)$$

$\bar{h}^{\circ}f$ is the standard enthalpy of formation at 25°C and 1 atm, whereas $(\bar{h} - \bar{h}^{\circ})$ is the enthalpy relative to the standard reference state.

Since the changes in kinetic and potential energy are negligible, the steady-flow energy equilibrium relationship $\dot{E}_{in} = \dot{E}_{out}$ can be expressed in the energy balance for a steady-flow system that reacts chemically more explicitly as:

$$\dot{n}_{FeCl_2}(\bar{h}^{\circ}f + \bar{h} - \bar{h}^{\circ})_{FeCl_2} + \dot{n}_{HCl}(\bar{h}^{\circ}f + \bar{h} - \bar{h}^{\circ})_{HCl} + \dot{W}_{PEM} = \dot{n}_{FeCl_3}(\bar{h}^{\circ}f + \bar{h} - \bar{h}^{\circ})_{FeCl_3} + \dot{n}_{H_2}(\bar{h}^{\circ}f + \bar{h} - \bar{h}^{\circ})_{H_2} \quad (4)$$

The molar flow rate (ṅ) can be defined as:

$$\dot{n} = \frac{\dot{m}}{Mr} \quad (5)$$

Where ṁ and Mr are mass flow rate and molecular weight, respectively.

After formulating the energy balance equation for the process, the enthalpy values for $FeCl_2$, $FeCl_3$ and H_2 can be calculated using the following Shomate equation:

$$\bar{h} - \bar{h}^{\circ} = AT + B\frac{T^2}{2} + C\frac{T^3}{3} + D\frac{T^4}{4} - E\frac{1}{T} + F - H \quad (6)$$

T is 1/1000 of the compound temperature for the compound (in K) and A, B, C, D, E, F, G, and H are constants for $FeCl_2$, $FeCl_3$ and H_2 as presented in Table 1.

Table 1. Enthalpy of formation, standard entropy and Shomate constant for $FeCl_2$, $FeCl_3$ and H_2

	Compound		
	$FeCl_3$ (aq)	$FeCl_2$ (aq)	H_2 (g)
$h°_f$ (kJ/mol)	-362.82	-311.34	0
s^0 (kJ/mol K)	0.20066	0.13988	0.13068
A	133.888	102.1733	33.066178
B	0	-1.07882E-09	-11.363417
C	0	8.42401E-09	11.432816
D	0	-2.09674E-09	-2.772874
E	0	-1.84636E-10	-0.158558
F	-402.7343	-341.7989	-9.980797
G	362.6829	263.5223	172.707974
H	-362.8156	-311.3365	0

Source: [28]

Enthalpy value of HCl (aq) can be calculated using the following equation [29]:

$$\bar{h} - \bar{h}^{\circ} = \int_{Treff}^{T} Cp\ (T - T_{reff}) \quad (7)$$

In the electrolysis process, the rate of formation of H_2 gas can be defined as follows [30]:

$$\dot{n}_{H_2} = \frac{J}{2F} \quad (8)$$

J and F are the electric current density and Faraday's constant, respectively. The rate of electrical energy required by the electrolizer can be calculated by following equation:

$$\dot{W}_{PEM} = J_{PEM} . V_{PEM} \quad (9)$$

The voltage (V_{PEM}) can be calculated using the Nernst Equation:

$$V_{PEM} = {E^0}_{cell} - 2{,}303 \frac{R\,T}{n\,F} \log Q \quad (10)$$

${E^0}_{cell}$ value in this electrolysis process is 0.8 V [31]. n is moles of electrons exchanged in an electrochemical reaction, while Q denotes reaction quotient.

Based on the predetermined energy balance, energy efficiency can be calculated using the following equation:

$$\eta_{PEM} = \frac{\dot{n}_{FeCl_3}(\bar{h}^{\circ}f + \bar{h} - \bar{h}^{\circ})_{FeCl_3} + \dot{n}_{H_2}(\bar{h}^{\circ}f + \bar{h} - \bar{h}^{\circ})_{H_2}}{\dot{n}_{FeCl_2}(\bar{h}^{\circ}f + \bar{h} - \bar{h}^{\circ})_{FeCl_2} + \dot{n}_{HCl}(\bar{h}^{\circ}f + \bar{h} - \bar{h}^{\circ})_{HCl} + \dot{W}_{PEM}} \quad (11)$$

The steady flow entropy balance equation can be written as follows:

$$\dot{n}_{FeCl_2} s_{FeCl_2} + \dot{n}_{HCl} s_{HCl} + \dot{S}_{gen}^{PEM} = \dot{n}_{FeCl_3} s_{FeCl_3} + \dot{n}_{H_2} s_{H_2} \quad (12)$$

$\dot{S}_{gen}$ and s are increase in the entropy rate of the system and specific entropy, respectively.

Specific entropy values for each compound $FeCl_2$, $FeCl_3$ and H_2 can be calculated using the Shomate equation as follows:

$$s = A \ln(T) + BT + C\frac{T^2}{2} + D\frac{T^3}{3} - E\frac{1}{2T^2} + G \quad (13)$$

T is 1/1000 of the compound temperature for the compound (in K) and A, B, C, D, E, F, G, and H are constants for $FeCl_2$, $FeCl_3$ and H_2 obtained from Table 1.

Specific entropy value of HCl (aq) can be calculated using the following equation [29]:

$$s = s^0 + \int_{Treff}^{T} Cp \ln \frac{T}{T_{reff}} \quad (14)$$

Exergy associated with a process under certain circumstances is the sum of physical exergy and chemical exergy, as shown in the following equation:

$$ex = ex^{ph} + ex^{ch} \quad (15)$$

Ignoring the specific kinetic and potential exergy of the compound, the specific exergy can be calculated by the following equation:

$$ex = (h - h_0) - T_0(s - s_0) + ex^{ch} \quad (16)$$

The chemical exergy value is based on the reference exergy under standard conditions with the environment, T_0 = 25°C and P_0 = 1 atm, which is called standard chemical exergy. Standard chemical exergy for $FeCl_2$, $FeCl_3$, HCl and H_2 can be seen in Table 2.

Table 2. Standard chemical exergy for $FeCl_2$, $FeCl_3$, HCl and H_2 at T_0 = 298.15 K and P_0 = 1 atm

Compound	$\overline{ex}^{ch}$ (kJ/mol)
$FeCl_2$	193,1
$FeCl_3$	225,6
HCl	84,5
H_2	236,1

Source: [32]

The exergy of the destruction ($\dot{E}x_D^{PEM}$) can be calculated as follows:

$$\dot{E}x_D^{PEM} = T_0 \times \dot{S}_{gen} \quad (17)$$

The exergy balance for a chemically reacting steady-flow system is more explicitly stated as:

$$\dot{n}_{FeCl_2} ex_{FeCl_2} + \dot{n}_{HCl} ex_{HCl} + \dot{E}x^{W}_{PEM} = \dot{n}_{FeCl_3} ex_{FeCl_3} + \dot{n}_{H_2} ex_{H_2} + \dot{E}x^{PEM}_{D} \quad (18)$$

$$\dot{E}x^{W}_{PEM} = \dot{W}_{PEM} \quad (19)$$

The exergy efficiency of the electrolyzer can be calculated as follows:

$$\Psi_{PEM} = \frac{\dot{n}_{FeCl_3} ex_{FeCl_3} + \dot{n}_{H_2} ex_{H_2}}{\dot{n}_{FeCl_2} ex_{FeCl_2} + \dot{n}_{HCl} ex_{HCl} + \dot{W}_{PEM}} \quad (20)$$

Furthermore, the hydrogen energy produced ($\dot{E}_{hidrogen}$) can be calculated by the following equation:

$$\dot{E}_{hidrogen} = \dot{m}_{H_2} \times LHV_{H_2} \quad (21)$$

RESULT AND DISCUSSION

Production of hydrogen from H_2S through the indirect electrolysis method, Fe-Cl hybrid was analyzed thermodynamically using some assumptions described previously. The thermodynamic analysis of the electrolyzer was carried out using the mass, energy and exergy balance equations for chemically reacting steady flow systems as described in the previous section. Thermodynamic calculations are performed manually using Microsoft Excel to determine the effect of several predetermined independent variables on the required electrical energy, energy efficiency and exergy, entropy generation rate, and exergy destruction. H_2S mass flow rate data was obtained through direct measurements at one of the GPP located in North Sumatra Province, Indonesia.

A. Effect of H_2S mass flow rate and electrolysis temperature on the electricity required

Electricity required to produce hydrogen from H_2S is 20.57 kWh/kg H_2. This shows that the energy required to decompose H_2S is less than to decompose water [13], [15] which theoretically requires energy of 32.68 kWh/kg H_2 [9], [33]. As the mass flow rate of H_2S rises, so does the demand for electricity (Figure 2a). This is due to the fact that a higher H_2S mass flow rate reduces mass transfer resistance and increases mass transfer rate. These alterations quicken the reaction rate, resulting in a higher demand for electricity. The mass flow rate of H_2S is the quantity of H_2S supplied per unit of time to the electrolysis process. It has an immediate impact on the quantity of electricity required for the electrolysis reaction. When more H_2S is introduced into the electrolyzer, more H_2S molecules must dissociate into hydrogen and sulfur ions [34]. This dissociation process requires the addition of electrical energy to disrupt the H_2S molecules' chemical bonds [35]. As a result, an increased flow rate of H_2S necessitates a higher electrical current to facilitate the dissociation reaction, resulting in a greater demand for electricity.

In contrast, as the electrolysis temperature rises, the amount of electricity required decreases progressively (Figure 2b). The electrolysis temperature plays an important role in determining the quantity of electricity required for the process. Electrolysis is an endothermic process that requires the addition of electrical energy [36]. The electrical energy requirement is directly affected by the temperature of the electrolysis system. In electrolysis systems, higher temperatures can reduce the quantity of electrical energy required for the reaction. This is due to the fact that higher temperatures increase the thermal energy of the system, resulting in increased ion mobility and a quicker rate of reaction [37]. Consequently, the ions involved in the electrolysis process are able to move more readily, allowing the desirable chemical reactions to take place with less electrical input. In addition, as the temperature of the electrolyzer raises, the migration of ions within the electrolyzer increases, resulting in an increase in solution conductivity and a decrease in electrolytic cell resistance [19]. As a result, less electricity is required for the process. It is essential to note, however, that there is an optimal temperature range where significant electricity savings can be realized. Further temperature increases beyond this range may not result in substantial electricity savings or may even be detrimental due to increased resistive heating and other energy losses. In order to accomplish efficient electrolysis and reduce energy consumption, it is essential to strike the proper equilibrium and operate within the optimal temperature range.

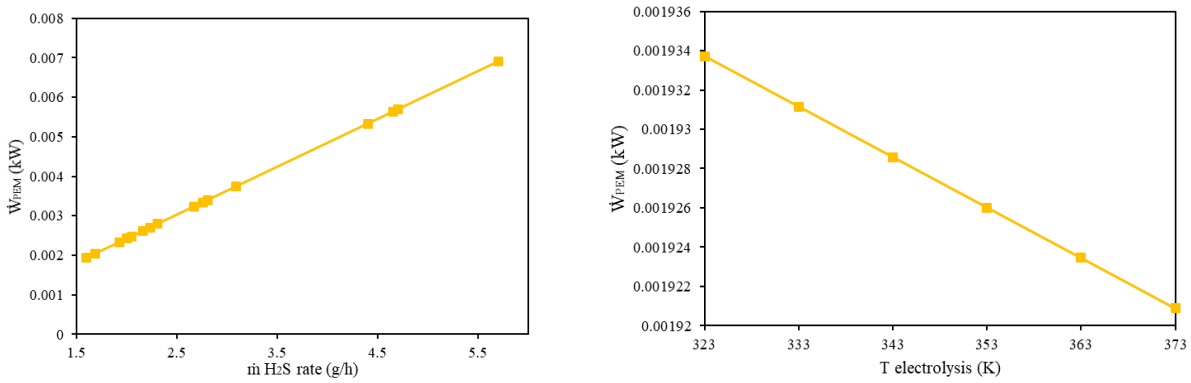

Figure 2. Effect of a) H_2S mass flow rate and b) electrolysis temperature on the electricity required

B. Effect of H_2S mass flow rate and electrolysis temperature on the exergy destruction

The mass flow rate of H_2S influences the exergy destruction during the electrolysis procedure. A greater mass flow rate results in a greater exergy destruction (Figure 3a). This is because the electrolyzer is supplied with a greater number of H_2S molecules per unit of time. These H_2S molecules must be dissociated into hydrogen and sulfur ions during electrolysis, a procedure that requires the application of electrical energy. Inefficiencies and losses within the electrolysis procedure contribute to exergy loss. With a greater H_2S mass flow rate, there is a greater demand for electricity and, as a result, a greater electrical current in the electrolyzer. This increased current can lead to greater resistive losses and inefficiencies, resulting in greater exergy loss. In addition, a higher mass flow rate of H_2S may increase mass transfer resistance and reduce the overall efficiency of the electrolysis process [19], thereby contributing further to exergy destruction. The rate of exergy destruction provides insight into the efficacy of the system [38]. By identifying the sources of exergy loss and working to reduce them, the system's effectiveness can be enhanced. Even with the most advanced technology, exergy destruction and losses are inevitable in a system. Exergy annihilation is caused by irreversible effects such as chemical reactions, the mingling of materials with various compositions or states, and friction [39]. Frictional effects become more significant as the mass flow rate increases, thereby accelerating the rate of exergy loss [40].

The electrolysis temperature influences the exergy destruction during the electrolysis procedure. Within a certain optimal temperature range, exergy destruction typically decreases as electrolysis temperature rises (Figure 3b). Higher temperatures have a number of beneficial effects on the system, resulting in enhanced efficacy and decreased losses. Enhanced ion mobility and accelerated reaction rates constitute a significant advantage of higher temperatures. This increased mobility permits the ions involved in the electrolysis process to move more readily, thereby reducing resistive losses and enhancing the performance of the electrolytic cell [41]. The higher temperature also enhances the system's thermal energy, which increases ionic mobility and accelerates reactions. Consequently, less electrical energy is squandered, resulting in less exergy destruction. In addition, higher temperatures can enhance the electrolyte's conductivity and the system's kinetic rate, thereby decreasing system losses [19]. This contributes further to the reduction of exergy loss. It is essential to note, however, that there exists an optimal temperature range beyond which further increases may result in diminishing returns or even be detrimental to the system. Extremely high temperatures can result in additional losses, including an increase in resistive heating, thermal radiation losses, and material degradation [42], [43]. These factors may outweigh the benefits of enhanced ion mobility, leading to an increase in exergy destruction. Therefore, it is essential to discover the optimal temperature range for electrolysis in order to maximize efficiency and prevent excessive temperature-related losses.

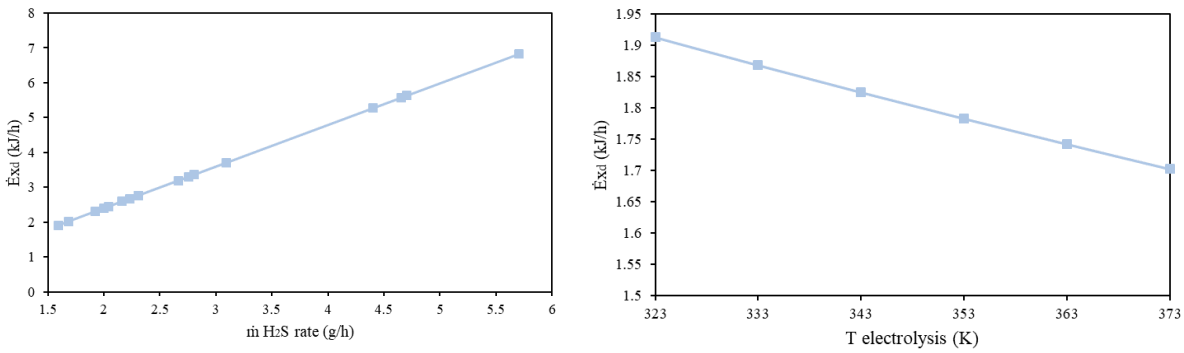

Figure 3. Effect of a) H_2S mass flow rate and b) electrolysis temperature on the exergy destruction

C. Effect of H_2S mass flow rate and electrolysis temperature on the entropy generation rate

An increase in mass flow rate generally results in an increase in the entropy generation rate (Figure 4a). When the mass flow rate of H_2S is higher, more H_2S molecules are supplied per unit of time to the electrolysis process. This increases the quantity of H_2S molecules that must dissociate during the electrolysis reaction into hydrogen and sulfur ions. The dissociation process requires the input of electrical energy, and any inefficiencies or losses contribute to the generation of entropy. A greater mass flow rate of H_2S results in a greater demand for electricity and, as a result, a greater electrical current in the electrolyzer. This increased current can lead to greater resistive losses and inefficiencies, which contribute to an increase in entropy production. In addition, a higher mass flow rate of H_2S may also increase the mass transfer resistance and decrease the overall efficiency of the electrolysis process, contributing further to the generation of entropy [19], [44]. The increased rate of mass transfer and reactions at higher mass flow rates can generate more irreversible processes, resulting in an increased rate of entropy production.

The effect of electrolysis temperature on the rate of entropy production is more complex. In general, the rate of entropy generation decreases as the electrolysis temperature rises up to a certain optimal range (Figure 4b). Higher temperatures can improve the mobility of ions, the conductivity of the electrolyte, and the reaction rates. This increased mobility and reaction rate results in increased efficiency and decreased entropy production [37], [44]. At higher temperatures, the system's thermal energy increases, allowing for greater ionic mobility and quicker reactions. This increased mobility allows the ions involved in the electrolysis process to move more readily, thereby reducing resistive losses and enhancing the performance of the electrolytic cell. As a consequence, less electrical energy is lost, resulting in decreased entropy production. Beyond the optimal temperature range, however, further increases in electrolysis temperature may enhance the rate of entropy production. Extremely high temperatures can result in additional losses, such as increased thermal radiation losses and material degradation, which can outweigh the benefits of enhanced ion mobility [42], [43]. These variables may contribute to an increase in entropy production and a decrease in efficiency.

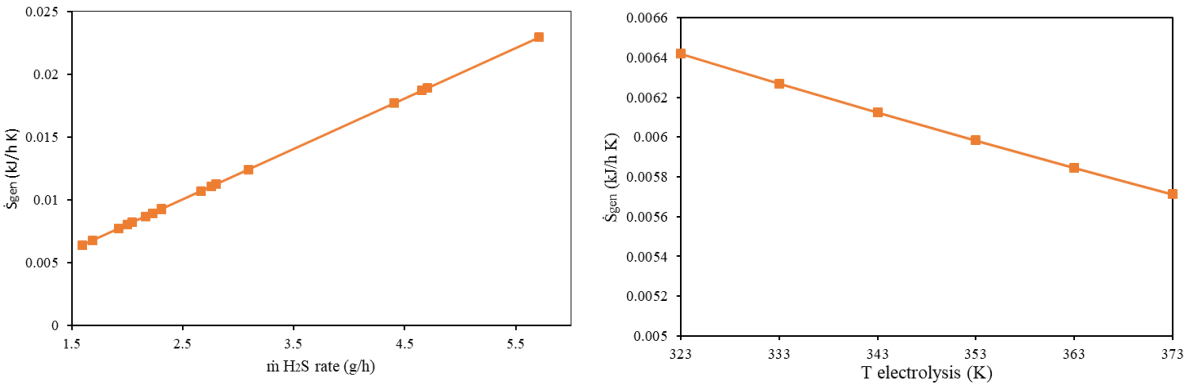

Figure 4. Effect of a) H_2S mass flow rate and b) electrolysis temperature on the entropy generation rate

D. Effect of H_2S mass flow rate and electrolysis temperature on the energy and exergy efficiency

Despite an increase in the H_2S mass flow rate, the electrolyzer's consistent energy and exergy efficiencies of 89.89% and 97.72%, respectively, indicate that the electrolysis process is operating efficiently within the investigated range of H_2S flow rates (Figure 5a). The observed consistency in efficacy suggests that the electrolyzer is likely operating near its optimal H_2S flow rate conditions. It implies that the system has been designed and optimized to accommodate a range of H_2S discharge rates without compromising its overall efficacy. Through meticulous design and engineering of the electrolyzer's components and system parameters, it is possible to attain optimal operating conditions. This may involve the selection of suitable materials, electrode configurations, and operating parameters such as temperature and pressure. Despite variations in the H_2S mass flow rate, the electrolyzer can maintain high efficiency by operating close to optimal conditions.

Increasing the temperature of electrolysis has a positive effect on the energy and exergy efficiencies, resulting in greater efficiency values (Figure 5b). The complex relationship between electrolysis temperature and energy or exergy efficiencies hinges on a number of variables. In general, increasing the electrolysis temperature increases both energy and exergy efficiencies within a certain optimal range [18]. Increased temperature increases the mobility of ions and accelerates reaction rates, resulting in increased efficiency [37]. The system's higher thermal energy enables greater ionic mobility, which facilitates more efficient ion movement during the electrolysis process [42]. This reduces resistive losses and increases the electrolytic cell's overall efficacy. Consequently, there is less electrical energy waste, resulting in greater energy and exergy efficiencies. The observed decrease in the rate of exergy destruction as the electrolyzer temperature increases confirms the decrease in system losses, which contributes to the system's increased efficiency. Compared to energy efficiency, exergy efficiency indicates a greater quality of energy utilized by the

system [45]. This demonstrates the enhanced sustainability of the system, as exergy analysis provides a comprehensive evaluation of energy degradation and precisely measures the actual work performed by the system [46].

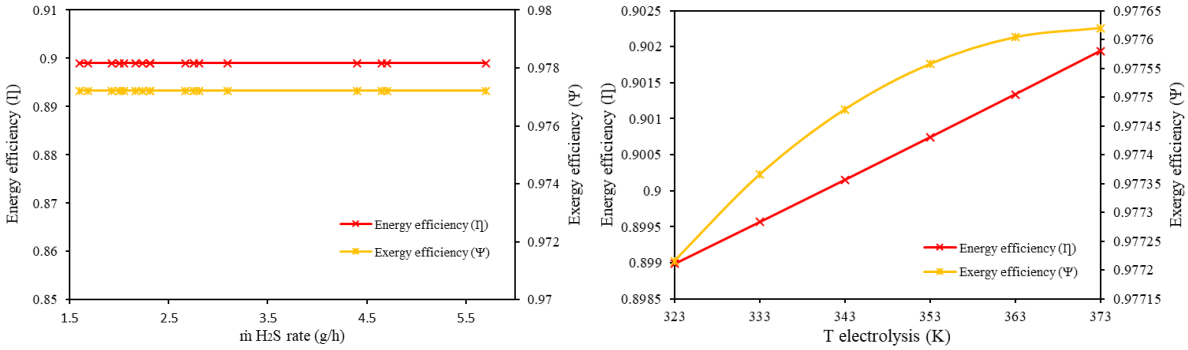

Figure 5. Effect of a) H_2S mass flow rate and b) electrolysis temperature on the energy and exergy efficiency

E. Hydrogen production in various H_2S mass flow rate

During electrolysis, the H_2S mass flow rate has a direct correlation with hydrogen production [18]. Greater H_2S emissions from a gas processing plant (GPP) can lead to increased hydrogen production. As depicted in the diagram below, an H_2S mass flow rate of 5.70 g/h at the location of the studied GPP can produce approximately 0.01 kW of hydrogen energy. The discharge rate of H_2S gas has a significant impact on the production of hydrogen during electrolysis. In this procedure, H_2S gas is introduced into an electrolysis cell with submerged anode and cathode electrodes. H_2S is oxidized at the anode, releasing electrons and forming sulfur, while water is reduced to produce hydrogen vapor. The discharge rate of H_2S affects the supply of H_2S molecules for oxidation at the anode. Higher flow rates increase the H_2S concentration at the anode, resulting in a greater number of reactant molecules and possibly a quicker reaction rate [19]. However, excessively high flow rates can limit mass transport and lead to concentration polarization [19]. When the diffusion rate of H_2S to the electrode surface becomes a limiting factor and slows the reaction rate, mass transport limitations occur. Concentration polarization is caused by the accumulation of reaction products near the anode's surface, which impedes contact with fresh H_2S and slows the reaction rate. Determining the optimal H_2S flow rate necessitates harmonizing the reaction rate, taking mass transport and other variables such as electrode material, cell voltage, temperature, and electrolyte composition into account [19], [25]. To minimize these effects and maximize the hydrogen production efficiency of a given system, it is vital to optimize the electrolysis cell design.

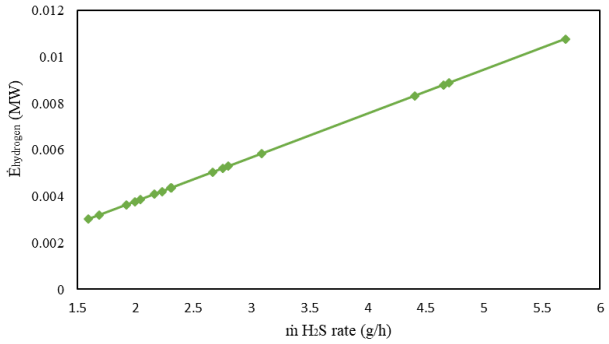

Figure 6. The relationship between the amount of hydrogen energy produced and the H_2S mass flow rate

CONCLUSION

This study examined the thermodynamic analysis of producing hydrogen from H_2S via indirect electrolysis. Analyses were conducted on the effects of H_2S mass flow rate and electrolysis temperature on various parameters. It was discovered that the mass flow rate of H_2S had a direct effect on the amount of electricity required for the electrolysis process. Higher flow rates increased the demand for electricity because more H_2S molecules required dissociation into hydrogen and sulfur ions. Increasing the electrolysis temperature, on the other hand, decreased the amount of electricity required because higher temperatures enhanced ion mobility and reaction rates. Electricity required to produce hydrogen from H_2S is 20.57 kWh/kg H_2. To avoid excessive losses, it is essential to operate within an optimal temperature range. The mass flow rate of H_2S also influenced the rates of exergy destruction and entropy

production, with higher flow rates resulting in greater exergy destruction and entropy production. In contrast, increasing the electrolysis temperature within the optimal range decreased exergy destruction and entropy production. Regardless of variations in the H_2S mass flow rate, the electrolyzer's energy and exergy efficiencies remained constant, indicating efficient operation within the investigated range. The energy and exergy efficiency of the electrolyzer are 89.89% and 97.72% respectively. Elevating the electrolysis temperature increased energy and exergy efficiencies even further. Hydrogen production was found to be directly proportional to the H_2S mass flow rate, with higher flow rates resulting in greater hydrogen production. For maximizing the efficiency of hydrogen production, it is essential to optimize the electrolysis cell design, considering variables such as electrode material, cell voltage, temperature, and electrolyte composition.

NOMENCLATURE

H_2S	:	Hydrogen sulfide
ORC	:	Organic Rankine Cycle
NCG	:	Non-Condensable Gas
PEM	:	Proton Exchange Membrane
LHV	:	Lower Heating Value
η	:	Energy efficiency
Ψ	:	Exergy efficiency
Ė	:	Energy (MW)
ex	:	Exergy
ex^{ch}	:	Chemical exergy (kJ/mol)
$\overline{ex}^{ch}$	:	Standard chemical exergy (kJ/mol)
ex^{ph}	:	Physical exergy (kJ/mol)
$\dot{E}x_d$	:	Exergy destruction (kW)
$\overline{h}^\circ_f$	:	Enthalpy of formation (kJ/mol)
$\overline{h}^\circ$	:	Standard enthapy (kJ/mol)
ṁ	:	Mass flow rate (g/h)
M	:	Molecular weight (g/mol)
ṅ	:	Molar flow rate (mol/h)
P	:	Pressure (MPa)
p	:	Product
r	:	Reactant
s°		Standard entropy (J/mol.K)
s	:	Specific entropy (J/mol.K)
$\dot{S}_{gen}$	:	Entropy generation rate (kW/K)
T	:	Temperature (K)
T_0	:	Ambient temperature (K)
Cp	:	Heat capacity (J/mol K)

ACKNOWLEDGMENTS

Author would like to thanks to the Center for Geothermal Research - Faculty of Science & Mathematics Undip and Bioelectrochemistry Research Group, Dept. of Chemistry Undip.

REFERENCE

[1] Kumar S, Himanshu SK, and Gupta KK, “Effect of Global Warming on Mankind-A Review,” 2012. [Online]. Available: www.isca.in

[2] S. C. Wijayasekera, K. Hewage, O. Siddiqui, P. Hettiaratchi, and R. Sadiq, “Waste-to-hydrogen technologies: A critical review of techno-economic and socio-environmental sustainability,” *International Journal of Hydrogen Energy*, vol. 47, no. 9. Elsevier Ltd, pp. 5842–5870, Jan. 29, 2022. doi: 10.1016/j.ijhydene.2021.11.226.

[3] A. Mostafaeipour, S. J. Hosseini Dehshiri, and S. S. Hosseini Dehshiri, “Ranking locations for producing hydrogen using geothermal energy in Afghanistan,” *Int J Hydrogen Energy*, vol. 45, no. 32, pp. 15924–15940, Jun. 2020, doi: 10.1016/j.ijhydene.2020.04.079.

[4] M. M. Hadjiat *et al.*, "Assessment of geothermal energy use with thermoelectric generator for hydrogen production," *Int J Hydrogen Energy*, vol. 46, no. 75, pp. 37545–37555, Oct. 2021, doi: 10.1016/j.ijhydene.2021.06.130.

[5] M. Aziz, "Liquid hydrogen: A review on liquefaction, storage, transportation, and safety," *Energies*, vol. 14, no. 18. MDPI, Sep. 01, 2021. doi: 10.3390/en14185917.

[6] M. E. Ramazankhani, A. Mostafaeipour, H. Hosseininasab, and M. B. Fakhrzad, "Feasibility of geothermal power assisted hydrogen production in Iran," *Int J Hydrogen Energy*, vol. 41, no. 41, pp. 18351–18369, Nov. 2016, doi: 10.1016/j.ijhydene.2016.08.150.

[7] M. Kanoglu, A. Bolatturk, and C. Yilmaz, "Thermodynamic analysis of models used in hydrogen production by geothermal energy," *Int J Hydrogen Energy*, vol. 35, no. 16, pp. 8783–8791, Aug. 2010, doi: 10.1016/j.ijhydene.2010.05.128.

[8] T. W. Hand, "Hydrogen Production Using Geothermal Energy," 2008. [Online]. Available: https://digitalcommons.usu.edu/etd

[9] G. K. Karayel, N. Javani, and I. Dincer, "Effective use of geothermal energy for hydrogen production: A comprehensive application," *Energy*, vol. 249, Jun. 2022, doi: 10.1016/j.energy.2022.123597.

[10] S. M. Alirahmi, E. Assareh, N. N. Pourghassab, M. Delpisheh, L. Barelli, and A. Baldinelli, "Green hydrogen & electricity production via geothermal-driven multi-generation system: Thermodynamic modeling and optimization," *Fuel*, vol. 308, Jan. 2022, doi: 10.1016/j.fuel.2021.122049.

[11] U. Cardella, L. Decker, and H. Klein, "Roadmap to economically viable hydrogen liquefaction," *Int J Hydrogen Energy*, vol. 42, no. 19, pp. 13329–13338, May 2017, doi: 10.1016/j.ijhydene.2017.01.068.

[12] Y. H. Chan *et al.*, "Hydrogen sulfide (H2S) conversion to hydrogen (H2) and value-added chemicals: Progress, challenges and outlook," *Chemical Engineering Journal*, vol. 458. Elsevier B.V., Feb. 15, 2023. doi: 10.1016/j.cej.2023.141398.

[13] E. Stefanakos, B. Krakow, and J. Mbah, "Hydrogen Production from Hydrogen Sulfide in IGCC Power Plants Final Scientific /Technical Report," 2007.

[14] K. Petrov, S. Z. Baykara, D. Ebrasu, M. Gulin, and A. Veziroglu, "An assessment of electrolytic hydrogen production from H2S in Black Sea waters," *Int J Hydrogen Energy*, vol. 36, no. 15, pp. 8936–8942, Jul. 2011, doi: 10.1016/j.ijhydene.2011.04.022.

[15] S. Ouali, S. Chader, M. Belhamel, and M. Benziada, "The exploitation of hydrogen sulfide for hydrogen production in geothermal areas," *Int J Hydrogen Energy*, vol. 36, no. 6, pp. 4103–4109, Mar. 2011, doi: 10.1016/j.ijhydene.2010.07.121.

[16] Y. H. Chan *et al.*, "A state-of-the-art review on capture and separation of hazardous hydrogen sulfide (H2S): Recent advances, challenges and outlook," *Environmental Pollution*, vol. 314. Elsevier Ltd, Dec. 01, 2022. doi: 10.1016/j.envpol.2022.120219.

[17] M. Finster, C. Clark, J. Schroeder, and L. Martino, "Geothermal produced fluids: Characteristics, treatment technologies, and management options," *Renewable and Sustainable Energy Reviews*, vol. 50. Elsevier Ltd, pp. 952–966, Jun. 09, 2015. doi: 10.1016/j.rser.2015.05.059.

[18] A. Karapekmez and I. Dincer, "Modelling of hydrogen production from hydrogen sulfide in geothermal power plants," *Int J Hydrogen Energy*, vol. 43, no. 23, pp. 10569–10579, Jun. 2018, doi: 10.1016/j.ijhydene.2018.02.020.

[19] H. Huang, J. Shang, Y. Yu, and K. H. Chung, "Recovery of hydrogen from hydrogen sulfide by indirect electrolysis process," *Int J Hydrogen Energy*, vol. 44, no. 11, pp. 5108–5113, Feb. 2019, doi: 10.1016/j.ijhydene.2018.11.010.

[20] A. Bassani *et al.*, "H2S in geothermal power plants: From waste to additional resource for energy and environment," *Chem Eng Trans*, vol. 70, pp. 127–132, 2018, doi: 10.3303/CET1870022.

[21] A. G. De Crisci, A. Moniri, and Y. Xu, "Hydrogen from hydrogen sulfide: towards a more sustainable hydrogen economy," *International Journal of Hydrogen Energy*, vol. 44, no. 3. Elsevier Ltd, pp. 1299–1327, Jan. 15, 2019. doi: 10.1016/j.ijhydene.2018.10.035.

[22] R. Somma, D. Granieri, C. Troise, C. Terranova, G. De Natale, and M. Pedone, "Modelling of hydrogen sulfide dispersion from the geothermal power plants of Tuscany (Italy)," *Science of the Total Environment*, vol. 583, pp. 408–420, Apr. 2017, doi: 10.1016/j.scitotenv.2017.01.084.

[23] K. Jangam, Y. Y. Chen, L. Qin, and L. S. Fan, "Perspectives on reactive separation and removal of hydrogen sulfide," *Chemical Engineering Science: X*, vol. 11, Aug. 2021, doi: 10.1016/j.cesx.2021.100105.

[24] K. Vala Matthíasdóttir, "Removal of Hydrogen Sulfide from Non-Condensable Geothermal Gas at Nesjavellir Power Plant," 2006.

[25] R. A. Adewale, A. S. Berrouk, and S. Dara, "A process simulation study of hydrogen and sulfur production from hydrogen sulfide using the Fe-Cl hybrid process," *J Taiwan Inst Chem Eng*, vol. 54, pp. 20–27, Sep. 2015, doi: 10.1016/j.jtice.2015.03.018.

[26] M. Mahmoud, M. Ramadan, S. Naher, K. Pullen, M. Ali Abdelkareem, and A. G. Olabi, "A review of geothermal energy-driven hydrogen production systems," *Thermal Science and Engineering Progress*, vol. 22, May 2021, doi: 10.1016/j.tsep.2021.100854.
[27] Y. A. Cengel and M. A. Boles, *Thermodynamics: an Engineering Approach*, Fifth Edition. McGraw-Hill, 2006.
[28] "https://webbook.nist.gov/chemistry/," 2023.
[29] D. R. Gaskell, *Introduction to the Thermodynamics of Materials*, Fifth Edition. New York: Taylor & Francis, 2008.
[30] B. Tekkanat, Y. E. Yuksel, and M. Ozturk, "The evaluation of hydrogen production via a geothermal-based multigeneration system with 3E analysis and multi-objective optimization," *Int J Hydrogen Energy*, Mar. 2022, doi: 10.1016/j.ijhydene.2022.11.185.
[31] S. Mizuta *et al.*, "Hydrogen production from hydrogen sulfide by the iron-chlorine hybrid process," *Ind Eng Chem Res*, vol. 30, no. 7, pp. 1601–1608, Jul. 1991, doi: 10.1021/ie00055a028.
[32] "https://exergy-calculator.ricklupton.name/browser/substance/," Mar. 23, 2023.
[33] C. Yilmaz, M. Kanoglu, A. Bolatturk, and M. Gadalla, "Economics of hydrogen production and liquefaction by geothermal energy," in *International Journal of Hydrogen Energy*, Jan. 2012, pp. 2058–2069. doi: 10.1016/j.ijhydene.2011.06.037.
[34] A. Karapekmez and I. Dincer, "Thermodynamic analysis of a novel solar and geothermal based combined energy system for hydrogen production," *Int J Hydrogen Energy*, vol. 45, no. 9, pp. 5608–5628, Feb. 2020, doi: 10.1016/j.ijhydene.2018.12.046.
[35] J. Zaman and A. Chakma, "Production of hydrogen and sulfur from hydrogen sulfide," 1995.
[36] M. Shah, M. Prajapati, K. Yadav, and A. Sircar, "A review of the geothermal integrated hydrogen production system as a sustainable way of solving potential fuel shortages," *J Clean Prod*, p. 135001, Nov. 2022, doi: 10.1016/j.jclepro.2022.135001.
[37] W. Li, S. Garcia, and S. Wang, "Thermoelectric ionogel for low-grade heat harvesting," in *Low-grade thermal energy harvesting: advances in materials, devices, and emerging applications*, S. Wang, Ed., Matthew Deans, 2022, pp. 63–82.
[38] Y. E. Yuksel and M. Ozturk, "Thermodynamic and thermoeconomic analyses of a geothermal energy based integrated system for hydrogen production," *Int J Hydrogen Energy*, vol. 42, no. 4, pp. 2530–2546, Jan. 2017, doi: 10.1016/j.ijhydene.2016.04.172.
[39] T. Gundersen, "The Concept of Exergy and Energy Quality," 2011.
[40] G. Tsatsaronis and F. Cziesla, "Thermoeconomics," in *Encyclopedia of Physical Science and Technology*, Elsevier, 2003, pp. 659–680. doi: 10.1016/B0-12-227410-5/00944-3.
[41] A. A. AlZahrani and I. Dincer, "Thermodynamic and electrochemical analyses of a solid oxide electrolyzer for hydrogen production," *Int J Hydrogen Energy*, vol. 42, no. 33, pp. 21404–21413, Aug. 2017, doi: 10.1016/j.ijhydene.2017.03.186.
[42] S. Rashidi, N. Karimi, B. Sunden, K. C. Kim, A. G. Olabi, and O. Mahian, "Progress and challenges on the thermal management of electrochemical energy conversion and storage technologies: Fuel cells, electrolysers, and supercapacitors," *Prog Energy Combust Sci*, vol. 88, p. 100966, Jan. 2022, doi: 10.1016/j.pecs.2021.100966.
[43] X. Chen *et al.*, "Temperature and voltage dynamic control of PEMFC Stack using MPC method," *Energy Reports*, vol. 8, pp. 798–808, Nov. 2022, doi: 10.1016/j.egyr.2021.11.271.
[44] T. Chmielniak and L. Remiorz, "Entropy analysis of hydrogen production in electrolytic processes," *Energy*, vol. 211, Nov. 2020, doi: 10.1016/j.energy.2020.118468.
[45] M. Kanoglu, I. Dincer, and Y. A. Cengel, "Exergy for better environment and sustainability," *Environ Dev Sustain*, vol. 11, no. 5, pp. 971–988, Sep. 2009, doi: 10.1007/s10668-008-9162-3.
[46] I. Dincer and A. Abu-Rayash, "Sustainability modeling," in *Energy Sustainability*, Elsevier, 2020, pp. 119–164. doi: 10.1016/B978-0-12-819556-7.00006-1.